A ROBUST SPECKLE REDUCING ANISOTROPIC DIFFUSION

Clovis Tauber, Hadj Batatia and Alain Ayache

IRIT UMR CNRS 5505
ENSEEIHT, 2 rue Camichel, BP 7122 31071 Toulouse Cedex 7, France
{tauber, batatia, ayache}@enseeiht.fr

Abstract

This paper deals with anisotropic diffusion in images affected by speckle. Two existing methods are reviewed. The first is a robust diffusion technique, non adapted to speckle, based on the Tukey function. The second applies anisotropic diffusion to speckle but lacks robustness. The contribution of this paper is to create a robust anisotropic diffusion filter adapted to speckle. The proposed approach is based on the two reviewed methods and introduces an original diffusion tensor. Experimentation results are presented and the performance of the three methods compared. The proposed algorithm shows significant enhancement.

Keywords

Anisotropic diffusion, speckle, robust methods.

1. INTRODUCTION

Filtering images affected by speckle is required for many applications including medical imaging. Most widely used techniques to reduce speckle include the Lee filter [6], Frost filter [4], Kuan filter [5] and the Gamma Maximum a Posteriori (MAP) [7]. All these filters seek a balance between averaging and all-pass filters. In this paper we aim to enhance the quality of ultrasound images affected by speckle using an anisotropic diffusion filter. This technique, introduced by Perona and Malik [8], has been widely studied [1, 3, 11, 12]. It performs well on images affected by additive noise, but tends to increase the noise when images contain speckle. Recently several works have aimed to improve the quality of anisotropic diffusion; Yu and Acton [13] have adapted this technique to reduce speckle, and Black [2] established the relationship between the diffusion equation and the robust estimation of a piecewise smooth image from noisy data. Our approach aims at creating a *robust speckle reducing anisotropic filter* based on the advantages of the methods of Yu and Black. The remainder of this paper is organized as follows. In section 2 we revisit classical anisotropic diffusion algorithm. We also present the recent techniques from which we have derived our algorithm. In section 3 we develop the proposed method. The experimentations are described in section 4.

2. ANISOTROPIC DIFFUSION TECHNIQUES

The anisotropic diffusion technique has been introduced by Perona and Malik [8]. The partial differential equation representing the diffusion is :

$$\begin{cases} \frac{\delta I}{\delta t} = \mathrm{div}[c(|\nabla I|).\nabla I] \\ I(t=0) = I_0 \end{cases} \quad (1)$$

where $c : \mathbf{R}^+ \rightarrow \mathbf{R}^+$ is called a diffusion tensor. One of the diffusion tensors introduced by Perona and Malik is :

$$c(x) = \frac{1}{1 + (x/k)^2} \quad (2)$$

where k is a constant that depends on the application. The main focus of this paper is to create a robust diffusion tensor optimized for speckle.

2.1. Robust anisotropic diffusion

Black developped a statistical interpretation of anisotropic diffusion [2]. He showed that anisotropic diffusion can be considered as a robust estimation of a piecewise smooth image with the relation :

$$c(x) \doteq \frac{\rho'(x)}{x} \quad (3)$$

where ρ represents a robust error norm. It is then easy to apply any robust error norm from litterature to anisotropic diffusion. Robust error norms in the diffusion eliminate the influence of outliers. The diffusion tensor (2) used by Perona and Malik is related to the Lorentz error norm, whereas Black uses the Tukey error norm. Using the relation between c and ρ, Black's diffusion tensor is written :

$$c(x, \sigma_e) = \begin{cases} \frac{1}{2}[1 - (\frac{x}{\sigma_e})^2]^2 & \text{if } |x| \leq \sigma_e \\ 0 & \text{otherwise} \end{cases} \quad (4)$$

This norm has a value of zero above the threshold σ_e, a scale defined with tools from robust statistics [2, 10], allowing to set the influence of neighbours to zero. As opposed to the Lorentz norm, this approach of diffusion does not modify a piecewise constant image where discontinuities between regions are significantly high.

2.2. Anisotropic diffusion adapted to speckle

Speckle is a multiplicative locally correlated noise. Yu and Acton [13] have defined a model of anisotropic diffusion tailored to this kind of noise. Earlier filters that aimed to reduce speckle, such as Lee [6] and Frost [4], are based on the *coefficient of variation*. Yu and Acton reused such a coefficient and applied it to anisotropic diffusion. They expressed the coefficient of variation as:

$$C_{i,j}^2 = \frac{I_{i,j}^2 + \frac{1}{|\eta_s|}\nabla^2 I_{i,j}^2}{(I_{i,j} + \frac{1}{|\eta_s|}\nabla^2 I_{i,j})^2} - 1 \tag{5}$$

They also established the *instantaneous* coefficient of variation, with $I_{i,j} > 0 \ \forall i,j$:

$$q(i,j;t)^2 = \frac{(\frac{1}{2})(|\nabla I|/I)^2 - (\frac{1}{16})(\nabla^2 I/I)^2}{[1 + (\frac{1}{4})(\nabla^2 I/I)]^2} \tag{6}$$

their diffusion coefficient is written as :

$$c(q) = \frac{1}{1 + \frac{q^2(i,j;t) - q_0^2(t)}{q_0^2(t)(1+q_0^2(t))}} \tag{7}$$

where $q_0(t)$ is the scale factor of speckle (see [13]). For ultrasonic images we can estimate $q_0(t)$ with :

$$q_0(t) \approx \exp(-\mu t) \tag{8}$$

where μ is a constant ($\mu \leq 1$) allowing to slow down the decrease of q_0 while iterating the algorithm.

The weakness of this method is its sensitivity to outliers.

3. THE PROPOSED DIFFUSION TECHNIQUE

In this section we first present another way to compute the instantaneous coefficient of variation that reduces the complexity of our algorithm. Then we present our new technique which combines, in an original way, the anisotropic diffusion methods of Yu and Black. Our method has the advantages of being robust to outliers and adapted to speckle.

3.1. Instantaneous coefficient of variation

The instantaneous coefficient of variation (7) is used to differentiate homogeneous regions ($\frac{q}{q_0}$ is close to 1) from boundaries ($\frac{q}{q_0} \gg 1$). $|\nabla I_{i,j}|^2$ is discretized as the mean of $|\nabla_L I_{i,j}|^2$ and of $|\nabla_R I_{i,j}|^2$, with :

$$\nabla_L I_{i,j} = (I_{i,j} - I_{i-1,j}, I_{i,j} - I_{i,j-1})^T \tag{9}$$

$$\nabla_R I_{i,j} = (I_{i+1,j} - I_{i,j}, I_{i,j+1} - I_{i,j})^T \tag{10}$$

putting :

$$\begin{array}{l} I_{v_1} = I_{i-1,j}, I_{v_2} = I_{i,j+1} \\ I_{v_3} = I_{i+1,j}, I_{v_4} = I_{i,j-1} \end{array} \tag{11}$$

(6) can be rewritten :

$$q(i,j;t)^2 = \frac{\sum_{m=1}^{3}\sum_{n=m+1}^{4}(I_{v_m} - I_{v_n})^2}{(\sum_{m=1}^{4} I_{v_m})^2} \tag{12}$$

This expression of the coefficient of variation does not depend on the value of the central pixel of the window. It is a weighted mean of differences between all the pairs of neighbours of the current pixel.

In the next section we show how to introduce this coefficient in the Tukey norm resulting in a robust method. We also compare theoretically this method to those of Yu and Black.

3.2. The proposed tensor

Let R_2 be :

$$R_2 = \frac{q^2(i,j;t) - q_0^2(t)}{q_0^2(t)(1+q_0^2(t))} \tag{13}$$

For iteration t, R_2 depends on the image gradient at the pixel (i,j), on the parameter q_0, and on the image laplacian at pixel (i,j). This allows to detect boundaries not only with a high gradient amplitude, but also with a zero-crossing of the laplacian. Similarly to the ratio $(|\nabla(I)|/k)^2$, the ratio R_2 is higher on boundaries than in homogeneous areas. Thus it can be used as a parameter of the Tukey error norm:

$$c(q) = \begin{cases} \frac{1}{2}[1 - \frac{q(i,j;t)^2 - q_0(t)^2}{q_0(t)^2(1+q_0(t)^2)}]^2 & \text{if } \frac{q(i,j;t)^2 - q_0(t)^2}{q_0(t)^2(1+q_0(t)^2)} \leq 1 \\ 0 & \text{otherwise} \end{cases} \tag{14}$$

where the parameter q_0 should be adapted to the application.

In order to make a comparison between the diffusion coefficients, we scale our function as follows :

$$\begin{array}{l} a = 2\frac{(q_0^2+1)^3}{q_0^2(q_0^2+2)^2} \\ \tilde{c}(q) = ac(q). \end{array} \tag{15}$$

Figure 1 shows a comparison of the functions $c(q)$ used by Yu (thin line) and in our algorithm (thick line). These curves are associated to the first (1a) and the fortieth (1b) iterations. Our new function assigns zero weight to outliers corresponding to instantaneous coefficients of variation greater than $(q_0^4 + 2q_0^2)$. At the fortieth iteration the threshold is lower due to the decrease of q_0. The use of the Tukey function leads to a similar diffusion when q is small (i.e. in homogeneous areas). When q is higher, near a boundary, the value of our function is zero while the function of Yu decreases slowly. Hence the prediction of sharper boundaries obtained using our algorithm compared to Yu's.

In addition to enhancing the method of Yu, our algorithm performs better than the algorithm of Black which is not adapted to speckle since it uses exclusively the gradient amplitude.

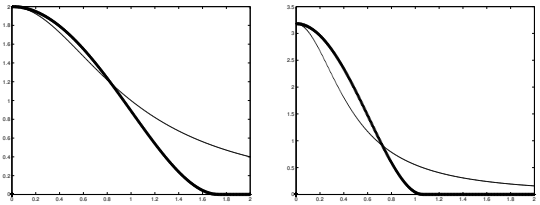

(a) (b)

Fig. 1. Comparison of the diffusion tensors

4. EXPERIMENTATION

4.1. Generating test images

In order to compare the algorithms, we have generated synthetic echographic images. We simulated the speckle with the model $x = s + s^{1/2}n$, where x is the observed signal, and s the original signal. n follows a zero mean, σ variance, gaussian law. This model is well suited for ultrasound images which have been manipulated numerous times (logarithmic compression, high pass and low pass filters, post treatment and other transforms).

4.2. Results

We evaluated the performance of our algorithm with several performance or feature indicators. We applied the algorithms both on the synthetic image described above and on an ultrasound image. A successful speckle filtering algorithm should reduce the variation within homogeneous regions and make sharper edges.

Method	FOM	NGM	MEAN
Noisy image	-	0.2313	187.2879
Perona-Malik	.6378	0.3601	187.5587
Black	.5157	0.2089	187.3169
Yu-Acton	.8790	0.4637	187.4586
Our algorithm	.9142	0.4874	187.3807

Table 1. Results on the synthetic image

Feature	Mean	SD	Sk	Ku	En
U. image	35.17	6.83	76.99	4.85e3	3.12e5
Yu-Acton	35.19	4.89	-19.97	1.23e3	3.02e5
Ours	35.20	4.47	-27.58	1.05e3	3.08e5

Table 2. Results on the ultrasound image (U. image)

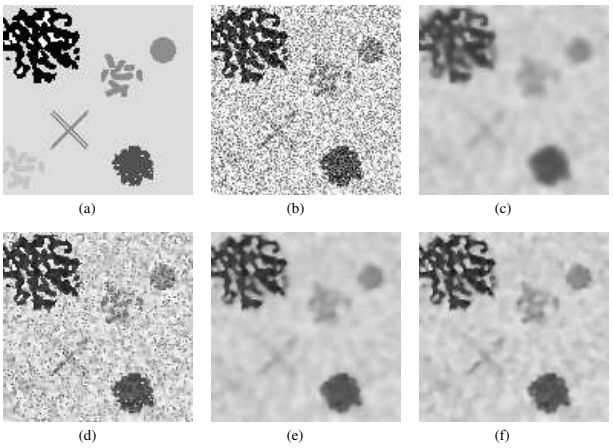

(a) (b) (c) (d) (e) (f)

Fig. 2. (a) Synthetic image, (b) Noisy image, and results for the algorithms of Perona (c), Black (d), Yu (e), and ours (f).

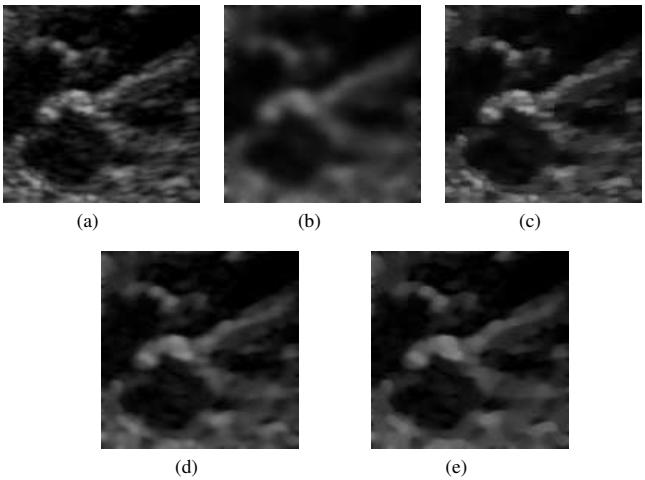

(a) (b) (c) (d) (e)

Fig. 3. (a) Ultrasound image, Results : (b) Perona, (c) Black, (d) Yu, and (e) ours.

On the synthetic image we have evaluated the performance using the classical Pratt's Figure Of Merit (FOM) [9], which measures the preservation of contours. We also used a performance indicator that we created : "Normalized Gradient Mean" (NGM). It is the ratio of the sum of the gradient amplitudes of edge pixels over the sum of the gradient amplitudes of all pixels of the image :

$$\text{NGM} = \frac{\sum_{s\in\zeta} |\nabla I_s|}{\sum_{s\in I} |\nabla I_s|} \tag{16}$$

with ζ the set of edge pixels. Edges were extracted on the initial synthethic image with a Sobel filter. NGM indicator is higher when the gradient amplitudes on edge are higher and when these amplitudes are lower inside homogeneous regions. Unlike FOM, it doesn't need an edge detection on

the result images. Table 1 shows the results. The FOM of our algorithm is slightly higher. Our algorithm also gets the best NGM score, while Black's score reflects that it is unadapted to speckle.

For the ultrasound image we measured several texture features: Mean, Standard Deviation (SD), Skewness (Sk), Kurtosis (Ku) and Entropy (En). These features evaluate mainly the quality of smoothing. The Mean was calculated on the entire image and shows that all tested filters are unbiaised. SD, Skewness and Kurtosis were calculated in a 32x32 window inside the right auricle. Table 2 shows the results. The Skewness and the Kurtosis are smaller in the filtered images. The Entropy also becomes smaller, depicting a loss of information in the filtered images. However the preserved Entropy corresponding to our algorithm is higher.

Figures 2c-2f show the results of Perona (c), Black (d), Yu (e) filters and ours (f) on the synthetic image (b), using 30 iterations, $\lambda = 0.05$ and $\mu = 1$. As predicted our algorithm leads to sharper edges. Figure 2d shows that the algorithm of Black is totally ineffective in presence of speckle.

Figure 3 shows the results on a real ultrasonic image (128x128 pixels) of a 12 weeks old foetus heart (3a) with the four filters tested on the synthetic data. We used 80 iterations, $\lambda = 0.03$ and $\mu = 1$. Note the smoothness of the homogeneous regions and the sharp edges given by our filter. Perona filter smoothes the image globally and Black's sharpen the edges everywhere even inside homogeneous regions, they are both inadapted to speckle. The filter of Yu is more suited to speckle but produces edges not as sharp as our filter.

5. CONCLUSION

This paper presented a new robust anisotropic diffusion technique adapted to speckle. This method is based on the work of Yu and Black and introduces an original diffusion tensor. Two factors have been considered when evaluating performance: contour preservation and smoothing quality. The FOM and NGM (a new quantitative performance indicator particularly adapted to diffusion) indicators were used to evaluate the first factor and Mean, Standard Deviation, Skewness, Kurtosis and Entropy for the second. The predicted analytical results are confirmed by experiments on both synthetic and real images. Results show that the proposed algorithm brings significant enhancement. Future work will im at taking into consideration the dynamics of motion during the diffusion process. Application to assisted echographic medical imaging is planned.

6. REFERENCES

[1] Alvarez L., Lions P-L, Morel J-M, "Image selective smoothing and edge detection by nonlinear diffusion", *SIAM Numer. Anal.*, Vol. 29(3), pp. 845-866, 1992.

[2] Black M. J., Sapiro G., Marimont D. H., Heeger D., "Robust anisotropic diffusion", *IEEE Trans. On Image Proc.*, Vol. 7, No 3, pp. 421-432, March 1998.

[3] Catte F., Lions P-L., Morel J-M., and Coll T., "Image selective smoothing and edge detection by nonlinear diffusion", *SIAM-JNA*, Vol. 29, pp 182-193, 1992

[4] Frost V. S., Stiles J. A., Shanmugan K. S., and Holtzman J. C., "A model for radar images and its application to adaptive digital filtering of multiplicative noise", *IEEE Trans. Pattern Anal. Machine Intell.*, Vol. PAMI-4, pp. 157-165, March 1982.

[5] Kuan D. T., Sawchuk A. A., Strand T. C., and Chavel P., "Adaptive restoration of images with speckle", *IEEE Trans. Acoust., Speech, Signal Processing*, Vol. ASSP-35, pp. 373-383, 1987.

[6] Lee J. S., "Digital image enhancement and noise filtering by using local statistics", *IEEE Trans. Pattern Anal. Machine Intell.*, Vol. PAMI-2, pp. 165-168, March 1980.

[7] Lopes A., Touzi R., and Nezry E., "Adaptive speckle filters and scene heterogeneity", *IEEE Trans. Geosci. Remote Sensing*, Vol. 28, pp. 992-1000, 1990.

[8] Perona P., Malik J., "Scale space and edge detection using anisotropic diffusion", *IEEE Trans. Pattern Anal. Machine Intell.*, Vol. 12, pp. 629-639, July 1990.

[9] Pratt W. K., "Digital Image Processing", *New York: Wiley*, 1977.

[10] Rousseeuw P. J., Leroy A. M., "Robust regression and outlier detection", *New York: Wiley*, 1987.

[11] Weickert J., "Anisotropic diffusion in image processing", *European Consortium for Mathematics in Industry (B.G. Teubner, Stuttgart).*, 1998.

[12] You Y. L., Xu W., Tannenbaum A., Kaveh M., "Behavioral analysis of anisotropic diffusion in image processing", *IEEE Trans. On Image Proc.*, Vol. 5, pp. 1539-1553, Nov 1996.

[13] Yu Y., Acton S. T., "Speckle reducing anisotropic diffusion", *IEEE Trans. On Image Proc.*, Vol. 11, No 11, pp. 1260-1270,Nov 2002.